

Determination of the Soil Water Characteristic Curve for Unsaturated Gypseous Soil from Model Tests

¹Mohammed Y. Fattah, ²Ahmed A.H. Al-Obaidi and ²Mohammed Kh.A. Al-Dorry

¹Department of Building and Construction Engineering, University of Technology, Baghdad, Iraq

²Department of Civil Engineering, University of Tikrit, Tikrit, Iraq

Abstract: The gypseous soil is a soil which has enough gypsum content to change or affect its engineering properties. Gypseous soils are usually stiff in their dry state due to the cementing action provided by gypsum but great loss of strength and pronounced increase in compressibility occur when gypsum is dissolved by partial or full saturation. This problem becomes more severe when the water flows through such soils causing loss of mass due to the leaching of gypsum. The soil used in this research is disturbed natural gypseous soil having three different percentages of gypsum; 55, 30 and 18%. Nine model tests were conducted to investigate the variation of suction, settlement and total vertical stress with time, also, study the effect of wetting on the volume change of unsaturated gypseous soil. The soil container used had with inner dimensions of (length 700×width 700×height 600 mm). A square footing of (100 mm) sides was used. Models in loose, medium and dense soils were prepared. Watermark monitor data logger model 900M was used to record the soil suction in kPa. The saturation process involved the complete saturation until the suction sensors readings approach to zero. The saturation process was established by allowing the water to infiltrate through the soil in upward-direction (from bottom to top of the model) with steady flow and head of 2 m. It was concluded that for soil with different gypsum contents, the air entry value decreases with the increase of the dry unit weight while the residual suction decreases slightly with the increase in dry unit weight. After reaching about 14.8 kN/m³, the residual suction starts to increase with the increase of dry unit weight. The residual water content decreases with the increase of gypseous content and soil density for all conducted tests.

Key words: Gypseous soil, collapsible, unsaturated, soil water characteristic curve, dry unit weight, soil density, gypseous content

INTRODUCTION

Gypseous soil is considered complicated with unpredictable behavior which makes it a problematic soil, gypseous soils attain high shear strength with very low compressibility at dry state but a sudden collapsible behavior appears when exposed to water.

Gypseous soil is intensified in arid and semi-arid regions. About 20-30% of the total area of Iraq is covered with gypseous soil. In Iraq, it has been recorded that several structures have faced different patterns of cracks and uneven deformations generated by exposing gypseous soil to water.

Changes of water content in gypseous content lead the gypsum which role as cementing agent to dissolve within the soil mass which results in one or combination of three processes, first breaking down of the bonds between soil particles supported by the gypsum followed by the collapse of soil structure and this process occurs almost immediately. The second process is consolidation while the third is leaching process which appears when

the water flow continues through the soil mass. The combination of these processes will cause the soil to settle considerably when loading is applied (Al-Nouri and Seleam, 1994).

Fattah *et al.* (2008) from test results on samples of gypseous soil having percentages of gypsum of 66, 44 and 14.8%, showed that the relationship between the vertical strain and logarithm of effective stress has two vertical lines. The first one represents the collapse settlement taking place within 24 h while the second one represents the long-term collapse. The collapse potential in both single and double oedometer tests increases significantly when the gypsum content increases from 14.8-66% and when the initial void ratio increases.

Mostly, collapsible soils are under unsaturated conditions in the dry state with negative pore pressure resulting in greater shear strength and higher effective stresses. The main geotechnical problem associated with these soils is the significant loss of shear strength and volume reduction happening when they are subjected to additional water from rainwater, irrigation, broken water or

sewer lines, moisture increase due to capillarity or “Pumping” as a result of traffic loading, ground water rises, etc.

Upon wetting, the pore pressure becomes less negative and the effective stresses are concentrated causing a decrease in shear strength. Furthermore, the water can dissolve or soften the bonds between the particles, permitting them to take a denser packing.

The Soil-Water-Characteristic-Curve (SWCC) has been used extensively for estimating unsaturated soil properties and a number of fitting equations for development of soil-water-characteristic-curves from laboratory data have been proposed by researchers such as Van Genuchten (1980), Fredlund and Xing (1994). The SWCC is a relationship between water content and suction of a soil. Hydraulically and physically, it means how much equilibrium water a soil can take at a given suction originally (Fredlund *et al.*, 2001).

Rodrigues and Vilar (2006) dealt with the influence of SWCC of an undisturbed sandy soil of collapse deformation. The results analyzed come from suction controlled oedometer tests and SWCCs. The results showed some features of the gradual collapse behavior of the tested soil and its relationship with the form and parameters of SWCC and present an empirical equation able to calculate the collapse potential development under matric suction variations using the parameters of the SWCC.

Aldaood *et al.* (2015) studied the SWCC of gypseous soil with (0, 5, 15 and 25%) gypsum content using tensiometric plate, osmotic membrane and vapor equilibrium techniques with suction pressure ranging between 10 and 1000000 kPa. The effect of two compaction efforts, standard and modified was examined on the SWCC of soil samples. The water holding capacity of soil samples increased with the increasing gypsum content and applied compaction effort. Mercury porosimetry tests and scanning electron microscope images revealed that compaction and presence of gypsum increased the number of capillarity pores. These changes in the pore size distribution of soil samples produced alterations in the volumetric water content at an Air-Entry Value (AEV) of the tested samples.

This study aims to evaluate the impacts of gypseous soil on the SWCC. Three soils of different gypsum contents are tested. Model tests are carried out through which the variation of soil matric suction was measured during the soil saturation by upward water flow.

MATERIALS AND METHODS

Description of the used soil: Three different disturbed natural gypseous soil samples were selected in this

research, Soil No. 1 from northern of Samarra City in Salah-Aldine governorate with high gypsum content (55%), Soil No. 2 from Abu Ghraib West of Baghdad City with medium gypsum content (30%) and Soil No. 3 from Abu Ghraib west of Baghdad city with medium gypsum content (18%).

In order to determine the required soil parameters, a soil-testing program was carried out at the soil mechanics laboratory of the university of technology in Baghdad. Routine soil tests were carried out to characterize the soil properties, namely the grain size analysis test, specific gravity, direct shear test, modified proctor compaction test and maximum and minimum dry density tests. The grain size distribution curve is shown in Fig. 1-3.

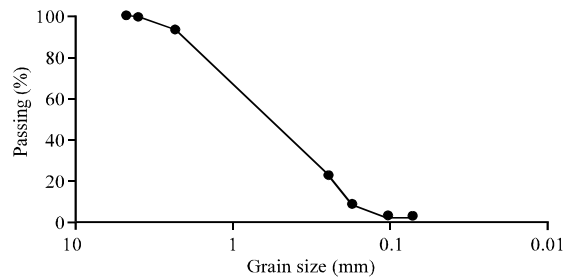


Fig. 1: Grain size distribution of soil No. 1 with 55% gypsum content

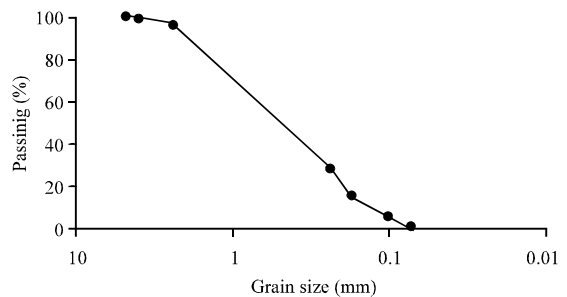


Fig. 2: Grain size distribution of soil No. 2 with 30% gypsum content

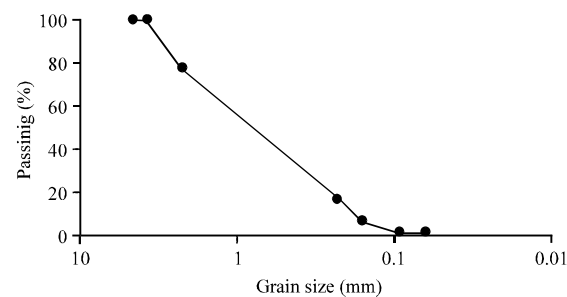


Fig. 3: Grain size distribution of soil No. 3 with 18% gypsum content

Table 1: Physical and mechanical properties of the used soils

Index property	Standards	Soil 1	Soil 2	Soil 3
Gypsum content (%)		55	30	18
Specific gravity (Gs)	ASTM D-854	2.36	2.54	2.61
D ₁₀ (mm)		0.18	0.13	0.2
D ₃₀ (mm)		0.31	0.27	0.4
D ₆₀ (mm)		0.8	0.7	1.15
Coefficient of uniformity (Cu)		4.4	5.4	5.8
Coefficient of curvature (Cc)		0.7	0.8	0.7
Maximum dry unit weight (kN/m ³)	ASTM D 4253-93	16.8	17.21	17.34
Minimum dry unit weight (kN/m ³)	ASTM D 4254-93	12	12	12
Soil classification according to (USCS)*	ASTM D 422-2001	SP	SP	SP
Friction angle	ASTM D 3080-7	38.1	36.3	36.1
Cohesion	ASTM D 3080-7	8	5	3

*USCS: Unified Soil Classification System

Table 2: Chemical properties of used soil

Chemical properties	Soil No. 1	Soil No. 2	Soil No. 3
Gypsum content (%)	55.00	30.00	18.00
Total sulphate content (SO ₃) %	25.50	13.90	8.40
pH value	8.25	8.31	8.28

Specific gravity tests were performed in accordance with Anonymous (2010) standard. Distilled water is normally used for specific gravity determination but Kerosene is recommended instead of distilled water when the soil specimens contain a significant fraction of organic matter or gypsum material (Anonymous, 2010). Specific gravity tests showed a decrease in G_s with the increase in gypsum content. This aspect of gypsum soils is important because G_s is directly associated with the unit weight of soils which is essential for all major geotechnical calculations. The mechanical and chemical properties of the soils used are summarized in Table 1 and 2.

The gypsum content calculated according to Al-Muftly and Nashat (2000). In this method an oven drying of the soil at 45°C will done until the weight of the sample becomes stable. The sample weight at 45°C is verified. Then, the sample is dried to 110°C until the weight becomes constant and recorded. The gypsum content is calculated according to the following equation:

$$x(\%) = \left[\frac{(W_{45^\circ c} - W_{11^\circ c})}{W_{45^\circ c}} \right] \times 4.778 \times 100$$

Where:

x = Gypsum content (%)

W_{45°C} = Weight of the sample at 45°C

W_{11°C} = Weight of the sample at 110°C

Table 3 shows the given name for the 9 model tests, simplified names are used for the explanations of the soil samples that will be dealt within in the experimental work, symbols are used to characterize each soil. Also, the data of the soil gypsum content, unit weight in the model and degree of saturation are mentioned.

Table 3: Simplified names for soil models in the tests

Test name	Gypsum content (%)	Dry unit weight (kN/m ³)	Degree of saturation (%)
A1	55	16.3	5.61
A2	30	16.3	4.80
A3	18	16.3	4.73
B1	55	14.8	4.18
B2	30	14.8	3.72
B3	18	14.8	3.58
C1	55	13.5	3.30
C2	30	13.5	3.00
C3	18	13.5	2.91

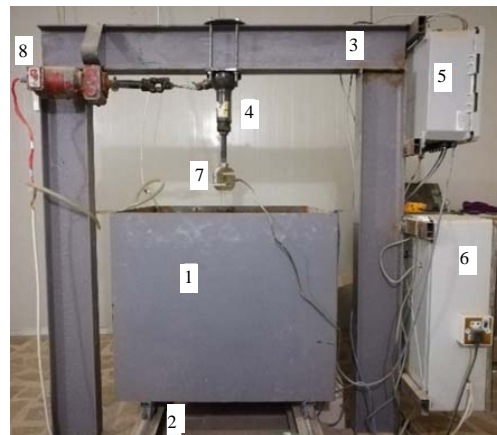


Fig. 4: Apparatus model used in tests: 1) Steel box; 2) Steel base; 3) Steel loading frame; 4) Axial loading system; 5) Geokon data logger; 6) Weight indicator and gearbox motor controller board; 7) Load cell sensor and 8) Gearbox motor

Description of experimental apparatus: The main parts of the apparatus were manufactured especially for this study by using of the available commercial material in the local market. Figure 4 shows the manufactured apparatus model, a schematic diagram of the experimental setup is presented in Fig. 5.

Two soil containers were used with inner dimensions of (length 700×width 700×height 600 mm) made as one piece of steel plate with 4 mm thickness. At the base of

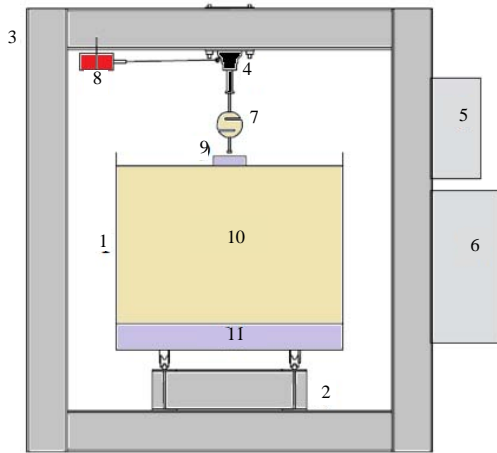


Fig. 5: Schematic diagram of the experimental setup: 1) Steel box; 2) Steel base; 3) Steel loading frame; 4) Axial loading system; 5) Geokon data logger; 6) weight indicator and gearbox controller; 7) Load cell sensor; 8) Gearbox motor; 9) Footing; 10) Soil bed and 11) Filter material

the two containers, four double sliding stainless steel sliding gate wheels pulley used to move the container under the loading frame.

A steel frame of 1350 mm height and 1000 mm width made of 4 inch (100 mm) I-section steel was manufactured. It was connected and pinned with 8 bolts to the middle of the steel base. In the superior horizontal beam of the frame, the axial loading system is connected and fixed.

The axial loading system consists of two base plates that were tied together by four 17 mm stainless steel bolts at the corners making the two plates easy to slip along the horizontal direction or fastened at desired location.

A square footing of 100 mm sides was used, it was made of three layers of plastic glasses each one is 10 mm thick glued together. The load was measured by a load cell.

Watermark monitor data logger model 900M was used to measure soil suction. The reading history provides a vivid picture of the soil suction profile. The watermark monitor data logger model 900M uses WaterGraph 3.2 Software (WG3). Automatically take reading from one a minute to one a day. The stored readings are transferred to a computer for display, the data file created can be opened by some spreadsheet or graphing programs including Microsoft Excel.

Model test preparation: Models in loose, medium and dense soils were prepared using an electrical steel tamping hammer manufactured for this purpose as shown in Fig. 6. The soils were prepared at three values of dry unit weight (16.3, 14.8 and 13.5 kN/m³), for each one of the three gypseous soil samples.



Fig. 6: Compacting soil model by modified jack hammer



Fig. 7: Filter material preparation

The bottom layer was overlain by a filter material used to allow free flow of water without soil erosion. This filter is compacted at a density equal to that of the soil sample. Two layers of geo-mesh were placed between the filter material and soil layer to prevent the mixing of the soil with filter material. Figure 7 shows the preparation of filter material. The zone of filter material has been determined according to the following steps mentioned by Das:

$$\frac{D_{15}(F)}{D_{85}(B)} < 5, \frac{D_{15}(F)}{D_{15}(B)} < 4, \frac{D_{50}(F)}{D_{50}(B)} < 25, \frac{D_{15}(F)}{D_{15}(B)} < 20$$

Where:

F = Filter material

B = Base soil

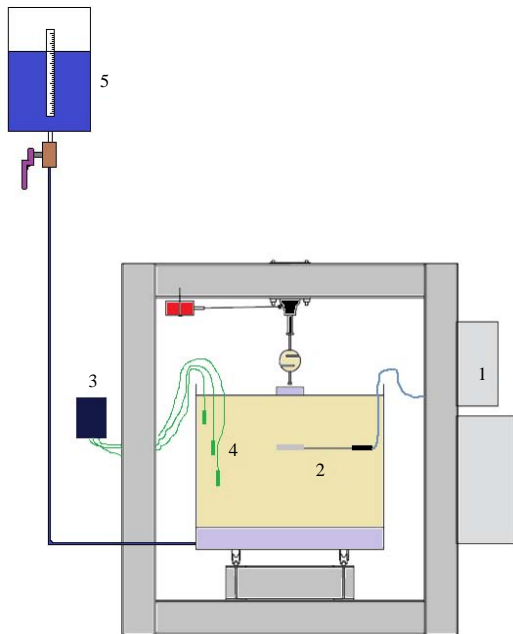


Fig. 8: Schematic diagram of the installed sensors and saturating system: 1) Geokon data logger; 2) Pressure cell sensor; 3) Irrometer watermark data logger; 4) Irrometer watermark sensors and 5) Saturating system

The weight required to achieve the unit weight and the volume of the container layers was predetermined. The soil was divided into equal weights, each weight represents the quantity of soil required for each layer.

The soil of each layer was compacted to a predetermined depth with the aid of modified jack hammer as presented in Fig. 6, each layer was scratched by a spatula in order to provide a good contact between the compacted layers.

The square footing was then placed in contact with the top surface of the model. The footing was centered under the loading rod on the surface of the soil. Two dial gauges of (0.01 mm) resolution were placed on two steel wings holder welded at the footing edges. The two dial gauges were attached to the sides of the container by two magnetic holders.

After that, the coring of the holes for Irrometer watermark sensors was prepared by using a jack hammer drilling machine attached to high quality Tungsten carbide cross head drill bits with dimensions (25 mm diameter and 500 mm length), then the final step was made with the use of the injection Irrometer tool CAT No. 1017. The installation of the sensors was carried out within three different holes at depths of 100, 200 and 300 mm at the sides of the container.

After-completing the model-set up, soil-saturation process was followed. The saturation process involved the complete saturation until the suction sensors readings approach to zero. The saturation process was performed by permitting the water to pass through the soil in upward-direction (from bottom to top of the model) with steady flow and head of 2 m. Figure 8 shows the schematic diagram of the installed sensors and the saturating system which has been used in model test.

RESULTS AND DISCUSSION

The wetting SWCC was obtained at large scale model by inserting three gypsum block sensors to 100, 200 and 300 mm depths from the surface footing for three gypseous soils with three different dry unit weights at the same initial water content. Figure 9-17 present the SWCC of soils obtained from 9 tests.

Fredlund and Xing (1994) stated that the soil-water-characteristic-curve consists of three stages which are: The boundary-effect zone where the pore-water is in tension but the soil-remains saturated. This stage ends at the air-entry value where the applied-suction dominates the capillary water-forces in the largest-pore in the soil.

The desaturation-zone where water is substituted by air-within the pore-spaces. This stage terminates at the residual-water content where the pore-water becomes discontinuous.

The residual saturation zone where water is tightly absorbed into the soil particles and flow happens in the form of vapor.

Table 4 presents the data extracted from the SWCC of air-entry value, residual suction and residual water content with the gypsum content for the nine soil models. Figure 18 shows the variation of the AEV with gypsum content, 19 presents the variation of residual suction with gypsum content while 20 presents the residual water content with gypsum. For Fig. 18 -20, the following points can be outlined:

For soil with gypsum content of 55%, the air entry value decreases with the increase of the dry unit weight while the residual suction decreases slightly with the increase in dry unit weight. After reaching about 14.8 kN/m³, the residual suction starts to increase with the increase of dry unit weight.

For soil with gypsum content of 30%, the air entry value increases with the increase of dry unit weight until reaching about 14.8 kN/m³, then starts to decrease with the increase of soil dry unit weight. For the residual suction, the increase of soil dry unit weight has no effect until reaching about 14.8 kN/m³, then a significant increase is observed as soil dry unit weight increase.

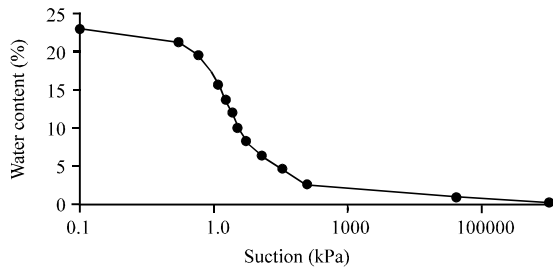


Fig. 9: SWCC for soil models A1 and D1

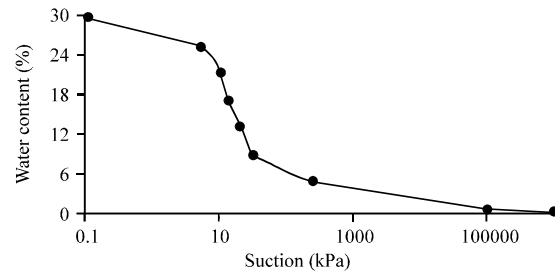


Fig. 13: SWCC for soil models B2 and E2

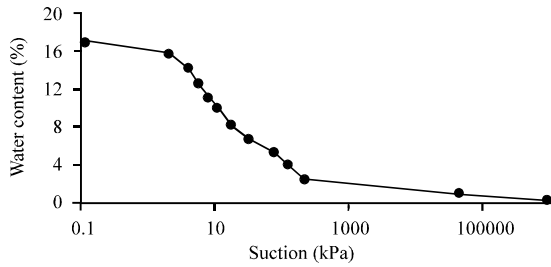


Fig. 10: SWCC for soil models A2 and D2

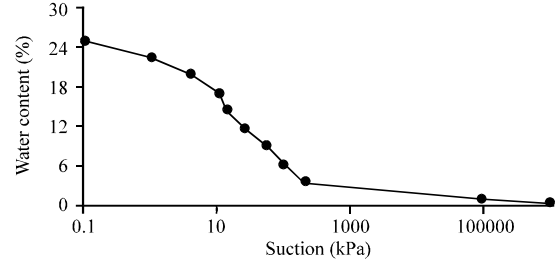


Fig. 14: SWCC for soil models B3 and E3

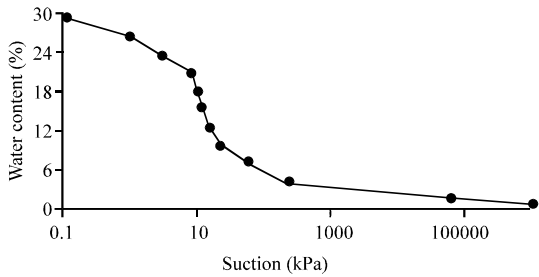


Fig. 11: SWCC for soil models A3 and D3

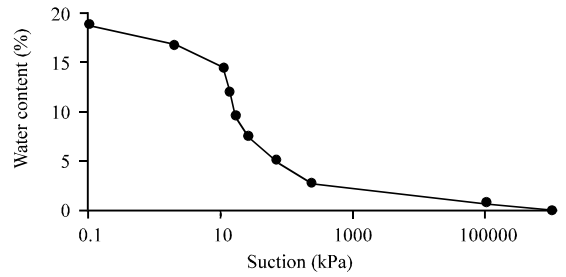


Fig. 15: SWCC for soil models C1 and F1

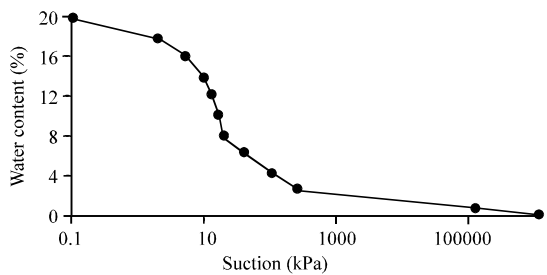


Fig. 12: SWCC for soil models B1 and E1

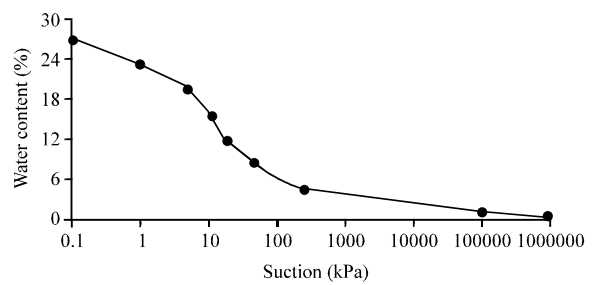


Fig. 16: SWCC for soil models C2 and F2

Table 4: Results of SWCC obtained from different soil models

Soil sample name	Gypsum content (%)	AEV (kPa)	Residual suction (kPa)	The residual water content (%)
A1	55	2.07	49	2.9
A2	30	4.90	31	3.6
A3	18	6.00	33	4.2
B1	55	4.05	67	3.3
B2	30	4.80	39	4.6
B3	18	3.30	33	5.7
C1	55	4.50	22	5.0
C2	30	5.00	37	6.2
C3	18	4.00	21	7.1

For soil with gypsum content of 18%, the air entry value increases with the increase of dry unit weight, then decreases with the increase of dry unit weight, the residual suction at first increases until reaching 14.8 kN/m³ dry unit weight then decreases.

The residual water content decreases with the increase of gypseous content and soil density for all conducted tests.

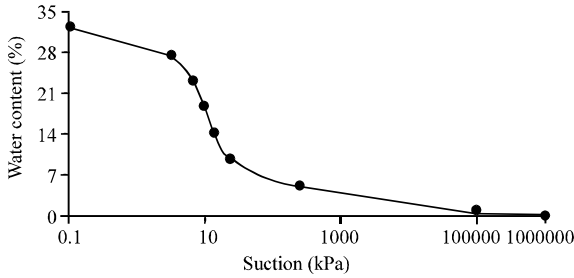


Fig. 17: SWCC for soil Models C3 and F3

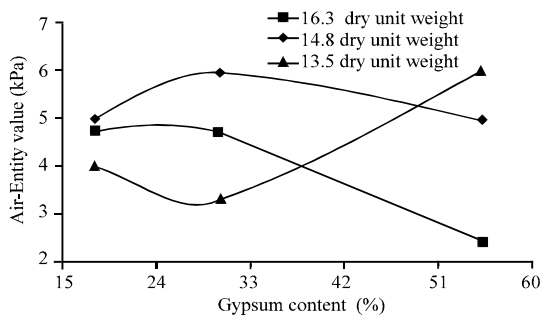


Fig. 18: Variation of the Air Entry Value (AEV) with gypsum content for different densities of soils

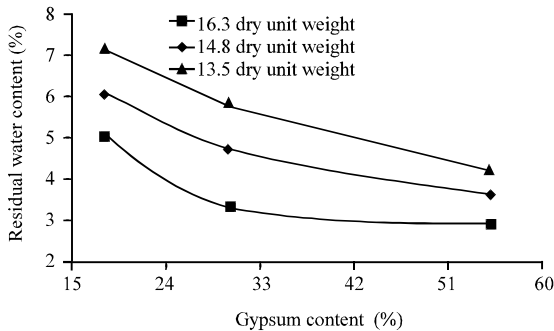


Fig. 19: Variation of the residual suction with gypsum content for soils of different densities

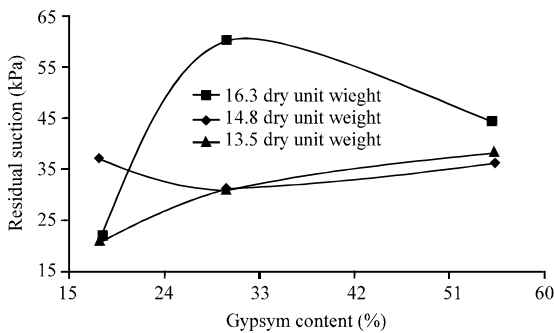


Fig. 20: Variation of the residual water content with gypsum content for soils of different densities

The AEV for soil with high density decreases slightly with the increase of gypsum content until reaching 30% gypsum content, then the AEV decreases with further increase in gypsum content. The AEV increases with the increase of gypsum content then decreases for moderate densities. For low soil density, the AEV decreases with the increase of gypsum content until reaching 30% then increases.

For high density soil with the increase of gypsum content, the residual suction increases then decrease while for moderate density soil, the residual suction decreases then increases with the gypsum content increase but for low density soils with the increase of gypsum content, the residual suction increases.

This behavior can be recognized to the effect of gypsum content on the grain-size distribution and then on the pore size distribution of these specimens. The gypsum content increase leads to increase in water content for a given suction value. Among the key parameters of the SWCC, the volumetric water content at the air-entry value is the one which changes the most because it depends directly on soil texture, in particular on the capillary pores, (Aldaood *et al.*, 2015).

In general, the matric suction value is controlled by the water content. When the water content decreases, the water menisci are withdrawn into smaller and smaller pore spaces, the radius of curvature of the menisci reduces and then the matric suction increases. The increase of matric suction leads to decrease of the driving potential for moisture flow and the increase of inter-particle contact stress, shear strength and shear modulus (Zhan, 2007).

Sheng and Zhou (2011) studied the impact of deformation on the soil-water-retention properties and found the impact of initial void ratio on the air-entry-value and the slope of SWCC. Therefore, the effect of initial dry density of soil should be sufficiently considered in estimating the SWCC of granular soils.

Generally speaking, the measured data are firstly needed to acquire the optimal curve-fitting parameters in the SWCC models. However, the measured data of SWCC and the fitting parameters attained high level of uncertainty due to the complicated un-modeled influencing factors (Zhou *et al.*, 2014).

Fattah *et al.* (2013) concluded that for the soil water characteristic curve which was determined by experimental method (i.e., filter paper method) for three soils from Baghdad, the matric suction value was found to increase with decrease of the degree of saturation and the rate of increase is not equal to the rate of decrease in degree of saturation. Also, the values of matric suction increases with decrease of the void ratio at the same degree of saturation.

Aldaood *et al.* (2014) found that osmotic suction, created by the presence of soluble gypsum in soil samples, caused additional water absorption. The changes in the engineering properties and behavior of soils due to a set of parameters including gypsum dissolution, pore size distribution and soil fabric changes revealed by XRD, SEM images and mercury porosimetry tests.

Moret-Fernandez and Herrero (2015) demonstrated that gypsum content has a sufficient influence on the soil-water-retention-curve WRC. Soils that had high gypsum content had WRC with higher water retention at near saturation conditions and steeper WRC slopes. The Equivalent Gypsum (EG) threshold at which gypsum influenced WRC was about 40%. Increasing EG values tend to increase and decrease the (a) and (n) Van Genuchten (1980) WRC parameters, respectively.

CONCLUSION

For soil with different gypsum contents, the air entry value decreases with the increase of the dry unit weight while the residual suction decreases slightly with the increase in dry unit weight. After reaching about 14.8 kN/m³, the residual suction starts to increase with the increase of dry unit weight.

The residual water content decreases with the increase of gypseous content and soil density for all conducted tests.

The AEV for soil with high density decreases slightly with the increase of gypsum content until reaching 30% gypsum content, then the AEV decreases with further increase in gypsum content. The AEV increases with the increase of gypsum content then decreases for moderate densities. For low soil density, the AEV decreases with the increase of gypsum content until reaching 30% then increases.

For high density soil with the increase of gypsum content, the residual suction increases then decrease, while for moderate density soil, the residual suction decreases then increases with the gypsum content increase but for low density soils with the increase of gypsum content, the residual suction increases.

REFERENCES

Al-Muftay, A.A. and I.H. Nashat, 2000. Gypsum content determination in gypseous soils and rocks. Proceedings of the 3rd Jordanian International Conference on Mining Amman Vol. 2, April 25-28, 2000, University of Jordan, Amman, Jordan, pp: 485-492.

Al-Nouri, I. and S. Saleam, 1994. Compressibility characteristics of gypseous sandy soils. *Geotech. Test. J.*, 17: 465-474.

Aldaood, A., M. Bouasker and M. Al-Mukhtar, 2014. Impact of Wetting-drying cycles on the microstructure and mechanical properties of Lime-stabilized gypseous soils. *Eng. Geol.*, 174: 11-21.

Aldaood, A., M. Bouasker and M. Al-Mukhtar, 2015. Soil-water characteristic curve of gypseous soil. *Geotech. Geol. Eng.*, 33: 123-135.

Anonymous, 2010. Standard test methods for specific gravity of soil solids by water pycnometer. ASTM International, West Conshohocken, Pennsylvania.

Fattah, M.Y., M.D. Ahmed and H.A. Mohammed, 2013. Determination of the shear strength, permeability and soil water characteristic curve of unsaturated soils from Iraq. *J. Earth Sci. Geotech. Eng.*, 3: 97-118.

Fattah, M.Y., Y.J. Al-Shakarchi and H.N. Al-Numani, 2008. Long-term behavior of a gypseous soil, engineering and technology journal. *Univ. Technol.*, 26: 1461-1483.

Fredlund, D.G. and A. Xing, 1994. Equations for the Soil-water characteristic curve. *Can. Geotech. J.*, 31: 521-532.

Fredlund, D.G., H. Rahardjo, L.C. Leong and C.W. Ng, 2001. Suggestions and recommendations for the interpretation of Soil-water characteristic curves. Proceedings of the 14th International Conference on Southeast Asian Geotechnical Vol. 1, December, 10-14, 2001, Hong Kong University of Science and Technology, Hong Kong, pp: 503-508.

Moret-Fernandez, D. and J. Herrero, 2015. Effect of gypsum content on soil water retention. *J. Hydrol.*, 528: 122-126.

Rodrigues, R. A. and O.M. Vilar, 2006. Relationship between Collapse and Soil-Water Retention Curve of a Sandy Soil. In: *Unsaturated Soils*, Miller, G.A., E.Z. Claudia, L.H. Sandra and G. F. Delwyn (Eds.). University of Michigan, Ann Arbor, Michigan, ISBN:9780784408025, pp: 1025-1036.

Sheng, D. and A.N. Zhou, 2011. Coupling hydraulic with mechanical models for unsaturated soils. *Can. Geotech. J.*, 48: 826-840.

Van Genuchten, M.T., 1980. A closed-form equation for predicting the hydraulic conductivity of unsaturated soils. *Soil Sci. Soc. Am. J.*, 44: 892-898.

Zhan, L., 2007. Soil-water interaction in unsaturated expansive soil slopes. *Front. Archit. Civil Eng. China*, 1: 198-204.

Zhou, L., X. Zhou, B. Zhang, M. Lu and Y. Luo *et al.*, 2014. Different responses of soil respiration and its components to nitrogen addition among biomes: A meta-analysis. *Global Change Biol.*, 20: 2332-2343.